

UCSF

UC San Francisco Previously Published Works

Title

Microarray gene expression analysis in ovine ductus arteriosus during fetal development and birth transition

Permalink

<https://escholarship.org/uc/item/76m9f62r>

Journal

Pediatric Research, 80(4)

ISSN

0031-3998

Authors

Goyal, Ravi
Goyal, Dipali
Longo, Lawrence D
[et al.](#)

Publication Date

2016-10-01

DOI

10.1038/pr.2016.123

Peer reviewed



Published in final edited form as:

Pediatr Res. 2016 October ; 80(4): 610–618. doi:10.1038/pr.2016.123.

Microarray gene expression analysis in ovine ductus arteriosus during fetal development and birth transition

Ravi Goyal¹, Dipali Goyal¹, Lawrence D. Longo¹, and Ronald I. Clyman²

¹Center for Perinatal Biology, Division of Basic Sciences, Loma Linda University, Loma Linda, California

²Department of Pediatrics and Cardiovascular Research Institute, University of California, San Francisco, California

Abstract

BACKGROUND—Patent ductus arteriosus (PDA) in the newborn is the most common congenital heart anomaly and is significantly more common in preterm infants. Contemporary pharmacological treatment is effective in only 70–80% of the cases. Moreover, indomethacin or ibuprofen, which are used to close a PDA may be accompanied by serious side effects in premature infants. To explore the novel molecular pathways, which may be involved in the maturation and closure of the ductus arteriosus (DA), we used fetal and neonatal sheep to test the hypothesis that maturational development of DA is associated with significant alterations in specific mRNA expression.

METHODS—We conducted oligonucleotide microarray experiments on the isolated mRNA from DA and ascending aorta from three study groups (premature fetus— 97 ± 0 d, near-term fetus— 136 ± 0.8 d, and newborn lamb— 12 ± 0 h). We compared the alterations in mRNA expression in DA and aorta to identify genes specifically involved in DA maturation.

RESULTS—Results demonstrate significant changes in wingless–integrin1, thrombospondin 1, receptor activator of nuclear factor-kappa B, nitric oxide synthase, and retinoic acid receptor activation signaling pathways.

CONCLUSION—We conclude that these pathways may play an important role during both development and postnatal DA closure and warrant further investigation.

The ductus arteriosus (DA) represents a persistence of the terminal portion of the sixth brachial arch. During fetal life, the DA serves to divert blood away from the fluid-filled lungs toward the descending aorta and placenta. After birth, constriction of the DA and obliteration of its lumen separate the pulmonary and systemic circulations. In full-term infants, obliteration of the DA takes place during the first 72 h after birth through a process of vasoconstriction and anatomic remodeling of ductus intima and media resulting in its permanent closure (1).

Correspondence: Ravi Goyal (rgoyal@llu.edu).

SUPPLEMENTARY MATERIAL

Supplementary material is linked to the online version of the paper at <http://www.nature.com/pr>

In contrast with the full-term newborn, in the preterm newborn the DA frequently fails to close. This is due to the pre-term ductus' limited ability both to actively vasoconstrict and reduce its luminal flow, as well as its limited ability to remodel its intimal/medial wall (1). When a patent ductus arteriosus (PDA) persists after birth, the blood shunts from the high-pressure aorta to the low-pressure pulmonary artery (left to right shunt). This can lead to pulmonary hyperemia and edema and decreases renal, mesenteric, and cerebral perfusion resulting in pulmonary engorgement with an increase in pulmonary vascular resistance and congestive cardiac failure. In those cases in which the pulmonary vascular resistance exceeds the systemic vascular resistance, the blood shunts from right to left. The main therapeutic option for a PDA is to treat the neonate with indomethacin or ibuprofen to inhibit the enzyme cyclooxygenase and thus inhibit prostaglandin synthesis. This is successful in about 70–80% of infants. Its use, however, may lead to undesirable side effects such as gastrointestinal bleeding, perforation, and/or necrotizing enterocolitis. If the PDA does not close by the age of 1–2 y, an operative closure (ligation or plug) is the only option for these infants. In full-term neonates, persistent PDA occurs in about 8 of 1,000 live births and makes up 5–10% of all congenital heart defects. Among preterm infants, the incidence of persistent PDA at the end of the first year is a several-fold higher.

At present the genes specific to the DA's developmental maturation *in utero* and associated with its postnatal anatomic closure are not known. Therefore, we tested the hypothesis that DA developmental transition is associated with differential gene expression. The aim of our study was to identify those genes and gene pathways that are altered during *both* developmental transitions (fetal maturation and postnatal closure) and whose alterations are unique to the DA. We examined gene expression profiles in DA and ascending aorta from premature fetal, near-term fetal, and newborn lambs using oligonucleotide microarray analysis. We compared the differential gene expression between the DA and ascending aorta to identify genes that are altered as a consequence of generalized vascular development and to differentiate them from genes specific for maturation of the DA.

RESULTS

Quality Check of Microarray Experiment

RNA purity of the study samples was between 1.8 and 2.0 ratio of OD_{260/280} as determined by UV spectrophotometry. Further quality of RNA was checked by Agilent Bioanalyzer (see Supplementary Figure S1 online), and the RNA integrity numbers were between 8.5 and 10. The RNA samples then were converted to cRNA targets and analyzed on Agilent Bioanalyzer. The electropherogram profiles (see Supplementary Figure S2 online) demonstrate high-quality cRNA. Intensity normalization was conducted following log transformation, and the probes above background were included in further analysis (see Supplementary Figure S3 online). Real-time PCR validation demonstrated that the fold-changes of the 12 genes examined were within 2 SDs of the values obtained by microarray experiment.

Developmental Changes in Gene Expression in DA and Aorta

To examine the genes exclusively regulated in DA during development and after birth, we compared the differences in gene expression (in the DA and aorta) between 97 ± 0 d and 136 ± 0.8 d gestational age fetuses, as well as between 136 ± 0.8 d gestation fetuses and newborn lambs (12 ± 0 h). Figure 1 presents the Venn diagrams of the genes that are differentially expressed in the three comparison groups from the DA (Figure 1a) and aorta (Figure 1b). As shown in the figure, with maturation of the fetus from 97 ± 0 to 136 ± 0.8 d, a total of 507 genes were altered significantly ($P < 0.05$; Figure 1a). Of these 507 genes, 213 genes were further changed after delivery (between 136 ± 0.8 d gestation age fetuses and newborn lambs) (Figure 1a). Similarly, in aorta 680 genes were altered significantly between 97 ± 0 and 136 ± 0.8 d gestation age fetuses ($P < 0.05$; Figure 1b), and 173 of these were further changed following delivery (Figure 1b).

Among the 213 genes that changed significantly in the DA during both developmental transitions (from 97 ± 0 to 136 ± 0.8 d gestation, and from 136 ± 0.8 d gestation to newborn), 102 genes were altered (>1.5 -fold; P value < 0.05) only in the DA but not in aorta (Figure 1c). Of these 102 genes, 93 correspond to known proteins (13 genes produce proteins localizing to the extracellular space, 16 genes produce proteins localizing to the plasma membrane, 30 genes produce proteins localizing to the cytoplasmic region, and 34 genes produce proteins localizing to the nucleus). Table 1 lists the top genes, which were exclusively altered (>2 -fold; P value < 0.05) in DA but not in aorta. We conducted real-time PCR to confirm the validity of the microarray by reexamining the mRNA expression levels of desmin, fibrinogen-like 2, fatty acid binding protein 4, serum amyloid A1, hairless homolog, basic helix-loop-helix family member e41, kelch domain containing 10, tumor necrosis factor receptor superfamily, member 13c, cell division cycle associated 7, paternally expressed 10, paternally expressed 3, and NIK related kinase. These are the top six upregulated and top six downregulated genes (Table 1). The expression levels were found to be highly correlated to the fold changes observed by microarray analysis.

Pathway Analysis on Altered Genes in DA With Maturation

We conducted Ingenuity Pathway Analysis on the 102 genes that were altered, specifically in the DA (and not in the aorta) during both developmental transitions. Figures 2 and 3 demonstrate the chief canonical and functional pathways, respectively, that are represented by the DA specific genes.

Network Analysis of Altered Genes

Using Ingenuity Pathway Analysis, we next examined the relationship between each of the DA specific gene, altered during both developmental transitions, with the other genes that were altered during the transitions. A network of direct and indirect interrelations among genes is shown Figure 4.

Upstream Regulator Analysis

The upstream regulator analysis identified several molecules, which can produce similar changes in gene expression as observed during the developmental transitions in the DA.

Some of the molecules were HIF1A, interleukin 1B, interleukin 2, and p38 MAPK inhibitor SB203580. A complete list is provided in Table 2.

Gene Annotation Based on Function

Next, we annotated the genes based on known function and cellular location. Among the main downregulated genes, were 2 cytokines, 12 transcriptional regulators, 4 extracellular ligands, and 8 membrane receptor components (Table 3). Similarly, upregulated genes contained 1 ion channel, a G protein-coupled receptor, 10 transcription factors, and 6 genes which participate in cell division (Table 4).

DISCUSSION

The DA continues to present significant challenges to preterm infants when it fails to close after birth. In this study, we identified several candidate genes that may be important in DA maturation, as they are altered during both fetal development and postnatal closure. To our knowledge, this is the first study to examine and compare the transcriptome of both DA and aorta in premature, near-term, and newborn sheep. Several transcriptomic studies have been reported previously in mice and rats; however, these have had different experimental designs or utilized single developmental time points for comparison, thereby limiting their ability to identify genes whose developmental changes are unique to the DA (2–6). A study in the rat examined changes in gene expression between DA and aorta at day 19 and 21 (3). We reanalyzed the microarray data from this study and compared it with the present study. We observed that 13 genes were commonly altered with maturation of only DA (not in aorta) in both this study and the study in rats (Table 5). A few of the top genes which were upregulated in both of these studies were phosphodiesterase 4B (PDE4B), desmin, pyruvate dehydrogenase kinase isozyme 4 (PDK4), and insulin-like growth factor binding protein 3 (IGFBP3). The downregulated genes were cyclin-dependent kinase inhibitor 1C (CDKN1C) and alpha-2-glycoprotein 1 (AZGP1). PDE4B limits the accumulation of cyclic AMP, which minimizes the vasodilating effects of endogenous prostaglandins within the ductus. An increase in PDE4B would facilitate DA constriction. Desmin is a marker of muscle cells and is an important cytoskeleton component. An increase in desmin with maturation may indicate a maturational increase in smooth muscle cells in the DA wall. PDK4 is known to regulate cell proliferation and apoptosis and may be important for DA closure (7). Furthermore, in our study, we observed an increase in transforming growth factor β -receptor II (TGFBR2). TGFBR2 is known to regulate PDK4 (8) and may play an important role in DA closure and remodeling (9).

Another interesting observation in this and other studies is the increased expression of IGFBP3. IGFBP3 overexpression is well known for induction of apoptosis (10–12). Apoptosis is an integral part of DA closure following birth, and these genes could play an important role in this process. Evidence also suggests that IGFBP3 is a downstream regulator of the wingless-integrin1 (Wnt) pathway. Based on our pathway analysis, the Wnt pathway appears to play a major role in DA (but not in the aorta) development and closure. Both canonical Wnt- β -catenin as well as the Wnt-PCP signaling pathway appear to be important in DA developmental transitions. A study in mice demonstrated that increased β -

catenin can lead to increased cyclooxygenase 2 and can lead to PDA (13). Cyclooxygenase inhibitors such as indomethacin and ibuprofen are presently used to close the PDA in preterm newborn. Moreover, β -catenin also can induce the expression of Ptg2 (which encodes cyclo-oxygenase-2) and stabilize its mRNA by interacting with AU-rich elements of the 3-un-translated region (14,15).

After delivery, macrophages play a crucial role in orchestrating cell death and remodeling of the newborn DA (16). Recent studies in similar vessels that undergo programmed cell death and remodeling during embryonic and fetal life have shown that this apoptotic process is mediated by macrophages via Wnt pathway (17). Of interest, the only G protein-coupled receptor altered (downregulated) with maturation specifically in ductus was frizzled class 2 receptor (FZD2). FZD2 is receptor for Wnt proteins and its activation leads to β -catenin accumulation. Thus, downregulation of FZD2 may be critical for ductus maturation and closure. However, a direct role of Wnt- β -catenin pathways in PDA closure remains to be evaluated by pharmacological agents.

Other than the Wnt pathway, this study identified several canonical pathways, which were altered significantly with developmental transitions in DA, but not in aorta. The top of the list included thrombospondin 1, receptor activator of nuclear factor-kappa B, nitric oxide synthase (NOS), and retinoic acid receptor (RAR) activation signaling pathways. Of these, there is substantial evidence for the involvement of retinoic acid pathway in DA maturation. In a transgenic mice study, intense activation of retinoic acid signaling was detected in DA during *in-utero* development (18). Importantly, such activation was absent in adjacent aortic or pulmonary arterial segments (18). Similarly, several other studies support the role of RAR in DA closure (19–21). However, further investigation is needed to determine the therapeutic potential of these pathways for treating PDA.

In this study, we observed upregulation of two cytokines: chemokine ligand 16 (CXCL16) and 8 (CXCL8). Notably, CXCL8 levels are known to be regulated by oxygen therapy in preterm infants (22). In addition, we observed upregulation of a number of transcription factors whose roles need to be evaluated. Similarly, we observed downregulation of several genes involved in cell division.

Perspective and Conclusion

Despite decades of research noninvasive options for closing a PDA remain limited. Accumulating evidence from microarray studies suggest that several genes and pathways involved with transcriptional regulation may have a unique role in the developmental transitions and closure of DA. A direct role of these pathways in DA closure needs to be demonstrated in future studies using pharmacological agents that can regulate these pathways. Fortunately, well-established pharmacological modulators are available for several of these pathways. This study provides support for experimental intervention that targets the Wnt and RAR, and perhaps other signaling pathways to determine their therapeutic potential for treating the PDA.

METHODS

Experimental Animals and Tissues

All experimental procedures were performed within the regulations of the Animal Welfare Act, the National Institutes of Health Guide for the Care and Use of Laboratory Animals, the Guidelines of the American Physiological Society and were approved by the Animal Care and Use Committee of Loma Linda University and the University of California, San Francisco.

We isolated DA and a segment of ascending aorta from preterm (97 ± 0 d gestation) and near-term (136 ± 0.8 d) fetal sheep (full term = 145 d) and from 12 ± 0 h old newborn lambs (obtained from Pozzi Ranch, Valley Ford, CA). Four animals ($n = 4$) were used for each experimental group. At the time of experimental study, ewes and newborn lambs were killed with an overdose of the proprietary euthanasia solution, Euthasol (pentobarbital sodium 100 mg/kg and phenytoin sodium 10 mg/kg; Virbac, Ft. Worth, TX).

Tissue Collection and Microarray Processing

In previous studies, we have described this technique in detail (23–25). Microarray analysis was conducted by utilizing the commercial services of GenUs BioSystems (Northbrook, IL). Briefly, DA and aorta segments (adjacent to DA) were homogenized and lysed in Trizol (Ambion, Austin, TX), and total RNA was isolated using phenol/chloroform extraction followed by purification over spin columns (Ambion). Total RNA concentration and purity of total RNA were measured by spectrophotometry at $OD_{260/280}$, and the quality of the total RNA sample was assessed using an Agilent Bioanalyzer (see Supplementary Figure S1 online) with RNA 6000 Nano Lab Chip (Agilent Technologies, Santa Clara, CA).

Labeled cRNA was prepared by linear amplification of the Poly(A) + RNA population within the total RNA sample. Briefly, <1 μ g of total RNA was reverse transcribed after priming with a DNA oligonucleotide containing the T7 RNA polymerase promoter 5' to a d(T)24 sequence. Following second-strand cDNA synthesis and purification of double-stranded cDNA, *in vitro* transcription was performed using T7 RNA polymerase. The quantity and quality of the labeled cRNA were assayed by spectrophotometry and Agilent Bioanalyzer.

One microgram of purified cRNA was fragmented to uniform size and applied to Agilent Sheep Gene Expression Microarray, 8×15 K (Design ID 019921, Agilent Technologies) in hybridization buffer. The arrays were hybridized at 65°C for 17 h in a shaking incubator and washed at 37°C for 1 min. Rinsed and dried arrays were scanned with an Agilent G2565 Microarray Scanner (Agilent Technologies) at 5 μ m resolution. Agilent Feature Extraction software was used to process the scanned images from arrays (gridding and feature intensity extraction), and the data generated for each probe on the array was analyzed with GeneSpring GX v7.3.1 software (Agilent Technologies). Annotations are based on the Agilent eArray annotation file dated January 2010.

Pathway/Network Analysis

The probes not annotated by the Agilent eArray annotation file were annotated manually using NCBI Blast Search, Unigene, Entrez, or other databases. We then analyzed the annotated genes using Ingenuity Pathway Analysis Program (Ingenuity Systems, Redwood City, CA).

Upstream Regulator Analysis

The goal of the upstream regulator analysis was to identify the signal transduction regulators that can mimic the observed gene expression changes in the present dataset with respect to the biological activities occurring in the tissues or cell system. Upstream regulator analysis was conducted using Ingenuity Pathway Analysis software. The direction of change in the gene expression observed in the experimental samples (relative to a control) was compared for changes in gene expression observed by application of a particular upstream regulator as published in the literature. Each potential upstream regulator was analyzed by using two statistical measures: an overlap *P* value and an activation *z*-score (23,26). The overlap *P* value was based on significant overlap between dataset genes and known targets regulated by an upstream regulator. The activation *z*-score was used to infer activation states of upstream regulators based on comparison with a model that assigns random regulatory directions (<http://ingenuity.force.com/ipa/servlet/fileField?id=0BE5000000PDow>).

Real-Time PCR Validation

Microarray analysis results were validated by real-time PCR. We chose the top six upregulated and six downregulated genes for analysis using real-time PCR. We designed primers using the same probe sequences as those on the microarray chip with the use of Primer 3 web-based software (<http://frodo.wi.mit.edu/primer3/>). The primers were synthesized by Integrated DNA Technologies (Coralville, CA). Total RNA (1 µg per reaction) was reverse transcribed using a QuantiTect Reverse Transcriptase Kit (Qiagen, Valencia, CA). Relative expression was normalized to 18S RNA and fold-changes were calculated using the cycle threshold method (27). Samples were analyzed on the LightCycler 1.5 (Roche, Indianapolis, IN).

Statistics

Individual expression values across arrays were compared by normalizing raw intensity data from each gene to the 75th percentile intensity of each array. Only genes with values greater than background intensity for all samples within each group were used for further analysis. Differentially expressed genes were identified by 1.5-fold change and Welch *t*-test *P* values <0.05 between each age and vessel group. Statistical significance in the real-time PCR data was determined by one-way ANOVA and *post-hoc* Newman–Keuls test.

Supplementary Material

Refer to Web version on PubMed Central for supplementary material.

Acknowledgments

STATEMENT OF FINANCIAL SUPPORT

This work was supported by grants from National Institute of Health, Bethesda, MD (HL109199 and HL46691 to R.I.C. and HD03807 to R.G.) and a gift from the Jamie and Bobby Gates Foundation, San Francisco, CA.

References

1. Clyman, RI. Mechanisms regulating closure of the ductus arteriosus. In: Polin, R.Fox, W., Abman, S., editors. *Fetal and Neonatal Physiology*. Philadelphia, PA: W.B. Saunders Co; 2011. p. 821-827.
2. Bökenkamp R, van Bremp R, van Munsteren JC, et al. Dlx1 and Rgs5 in the ductus arteriosus: vessel-specific genes identified by transcriptional profiling of laser-capture microdissected endothelial and smooth muscle cells. *PLoS One*. 2014; 9:e86892. [PubMed: 24489801]
3. Hsieh YT, Liu NM, Ohmori E, et al. Transcription profiles of the ductus arteriosus in Brown-Norway rats with irregular elastic fiber formation. *Circ J*. 2014; 78:1224–33. [PubMed: 24647370]
4. Jin MH, Yokoyama U, Sato Y, et al. DNA microarray profiling identified a new role of growth hormone in vascular remodeling of rat ductus arteriosus. *J Physiol Sci*. 2011; 61:167–79. [PubMed: 21287305]
5. Shelton EL, Ector G, Galindo CL, et al. Transcriptional profiling reveals ductus arteriosus-specific genes that regulate vascular tone. *Physiol Genomics*. 2014; 46:457–66. [PubMed: 24790087]
6. Liu NM, Yokota T, Maekawa S, et al. Transcription profiles of endothelial cells in the rat ductus arteriosus during a perinatal period. *PLoS One*. 2013; 8:e73685. [PubMed: 24086288]
7. Grassian AR, Metallo CM, Coloff JL, Stephanopoulos G, Brugge JS. Erk regulation of pyruvate dehydrogenase flux through PDK4 modulates cell proliferation. *Genes Dev*. 2011; 25:1716–33. [PubMed: 21852536]
8. Sun Y, Daemen A, Hatzivassiliou G, et al. Metabolic and transcriptional profiling reveals pyruvate dehydrogenase kinase 4 as a mediator of epithelial-mesenchymal transition and drug resistance in tumor cells. *Cancer Metab*. 2014; 2:20. [PubMed: 25379179]
9. Tannenbaum JE, Waleh NS, Mauray F, et al. Transforming growth factor beta 1 inhibits fetal lamb ductus arteriosus smooth muscle cell migration. *Pediatr Res*. 1995; 37:561–70. [PubMed: 7603772]
10. Han JJ, Xue DW, Han QR, et al. Induction of apoptosis by IGFBP3 overexpression in hepatocellular carcinoma cells. *Asian Pac J Cancer Prev*. 2014; 15:10085–9. [PubMed: 25556430]
11. Oikonomopoulos A, Sereti KI, Conyers F, et al. Wnt signaling exerts an antiproliferative effect on adult cardiac progenitor cells through IGFBP3. *Circ Res*. 2011; 109:1363–74. [PubMed: 22034491]
12. Wu YC, Buckner BR, Zhu M, Cavanagh HD, Robertson DM. Elevated IGFBP3 levels in diabetic tears: a negative regulator of IGF-1 signaling in the corneal epithelium. *Ocul Surf*. 2012; 10:100–7. [PubMed: 22482470]
13. Yajima I, Colombo S, Puig I, et al. A subpopulation of smooth muscle cells, derived from melanocyte-competent precursors, prevents patent ductus arteriosus. *PLoS One*. 2013; 8:e53183. [PubMed: 23382837]
14. Araki Y, Okamura S, Hussain SP, et al. Regulation of cyclooxygenase-2 expression by the Wnt and ras pathways. *Cancer Res*. 2003; 63:728–34. [PubMed: 12566320]
15. Lee HK, Jeong S. Beta-Catenin stabilizes cyclooxygenase-2 mRNA by interacting with AU-rich elements of 3'-UTR. *Nucleic Acids Res*. 2006; 34:5705–14. [PubMed: 17040897]
16. Waleh N, Seidner S, McCurmin D, et al. Anatomic closure of the premature patent ductus arteriosus: the role of CD14+/CD163+ mononuclear cells and VEGF in neointimal mound formation. *Pediatr Res*. 2011; 70:332–8. [PubMed: 21691249]
17. Kurihara T, Kubota Y, Ozawa Y, et al. von Hippel-Lindau protein regulates transition from the fetal to the adult circulatory system in retina. *Development*. 2010; 137:1563–71. [PubMed: 20388654]
18. Colbert MC, Kirby ML, Robbins J. Endogenous retinoic acid signaling colocalizes with advanced expression of the adult smooth muscle myosin heavy chain isoform during development of the ductus arteriosus. *Circ Res*. 1996; 78:790–8. [PubMed: 8620598]

19. Momma K, Toyono M, Miyagawa-Tomita S. Accelerated maturation of fetal ductus arteriosus by maternally administered vitamin A in rats. *Pediatr Res.* 1998; 43:629–32. [PubMed: 9585009]
20. Wu GR, Jing S, Momma K, Nakanishi T. The effect of vitamin A on contraction of the ductus arteriosus in fetal rat. *Pediatr Res.* 2001; 49:747–54. [PubMed: 11385133]
21. Wu LH, Xu SJ, Teng JY, Wu W, Ye DY, Wu XZ. Differential response of human fetal smooth muscle cells from arterial duct to retinoid acid. *Acta Pharmacol Sin.* 2008; 29:413–20. [PubMed: 18358086]
22. De Dooy J, Ieven M, Stevens W, De Clerck L, Mahieu L. High levels of CXCL8 in tracheal aspirate samples taken at birth are associated with adverse respiratory outcome only in preterm infants younger than 28 weeks gestation. *Pediatr Pulmonol.* 2007; 42:193–203. [PubMed: 17238187]
23. Goyal R, Longo LD. Acclimatization to long-term hypoxia: gene expression in ovine carotid arteries. *Physiol Genomics.* 2014; 46:725–34. [PubMed: 25052263]
24. Goyal R, Longo LD. Gene expression in sheep carotid arteries: major changes with maturational development. *Pediatr Res.* 2012; 72:137–46. [PubMed: 22565503]
25. Goyal R, Van Wickle J, Goyal D, Matei N, Longo LD. Antenatal maternal long-term hypoxia: acclimatization responses with altered gene expression in ovine fetal carotid arteries. *PLoS One.* 2013; 8:e82200. [PubMed: 24367503]
26. Dobyns AE, Goyal R, Carpenter LG, Freeman TC, Longo LD, Yellon SM. Macrophage gene expression associated with remodeling of the prepartum rat cervix: microarray and pathway analyses. *PLoS One.* 2015; 10:e0119782. [PubMed: 25811906]
27. Pfaffl MW. A new mathematical model for relative quantification in real-time RT-PCR. *Nucleic Acids Res.* 2001; 29:2002–2007.

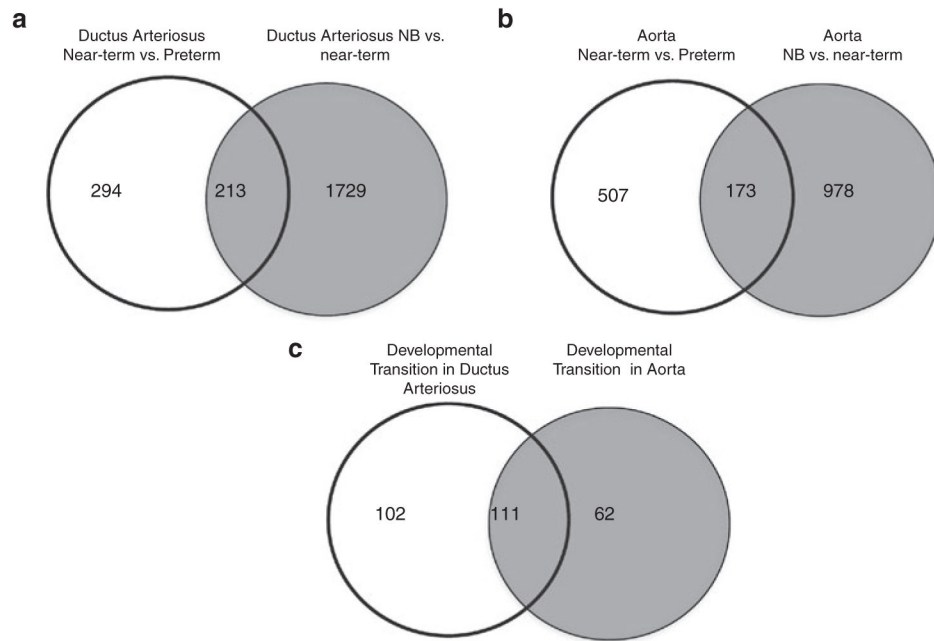


Figure 1. Venn diagram demonstrating differentially expressed genes in ovine ductus arteriosus. **(a)** Near-term vs. preterm and newborn (NB) vs. nearterm ductus arteriosus; **(b)** near-term vs. preterm and NB vs. near-term aorta; and **(c)** ductus and aorta with developmental transition from 97 ± 0 d fetus to 136 ± 0.8 d fetus, and NB lambs. The genes included are those which showed >1.5 -fold change in expression. $N = 4$ in each group; $P < 0.05$.

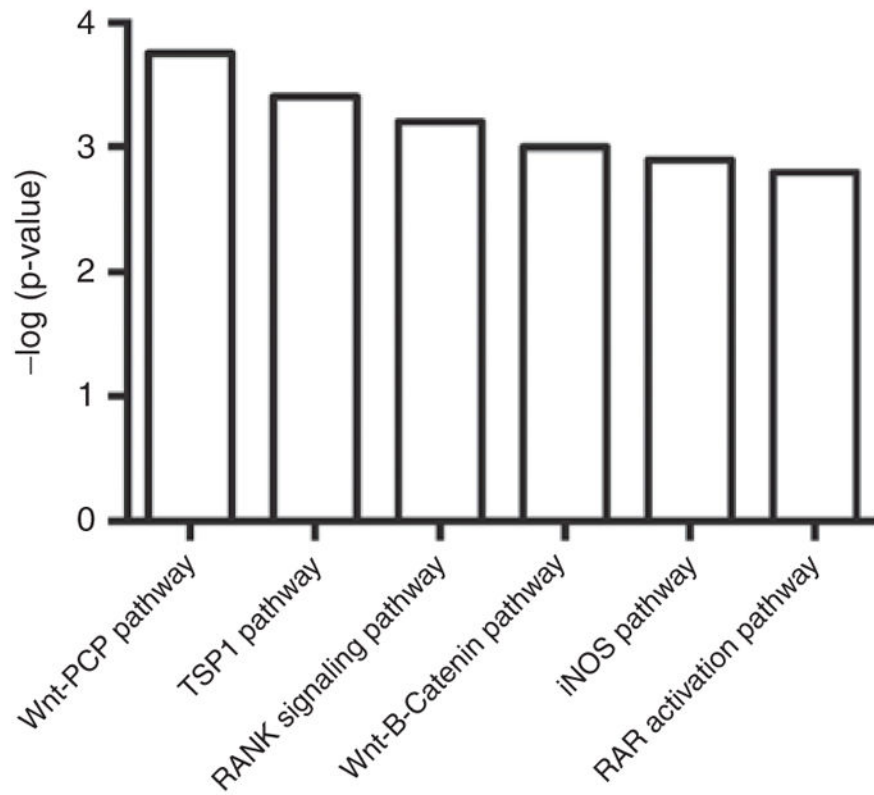


Figure 2.

Bar graphs demonstrate chief canonical pathways represented by the genes altered with maturation specifically in ductus arteriosus. The genes included are those which showed >1.5-fold change in expression. $N=4$ in each group; $P < 0.05$.

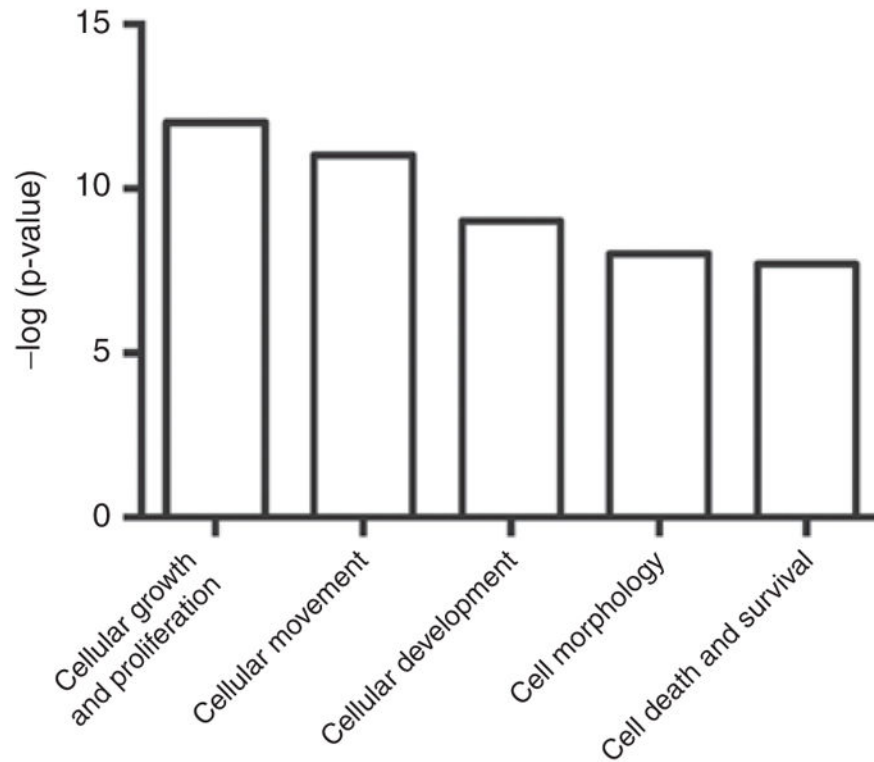


Figure 3.

Bar graphs demonstrate chief functional pathways represented by the genes altered during both developmental transitions (from 97 ± 0 to 136 ± 0.8 d gestation, and from 136 ± 0.8 d gestation to newborn), specifically in ductus arteriosus. The genes included are those which showed >1.5-fold change in expression. $N = 4$ in each group; $P < 0.05$.

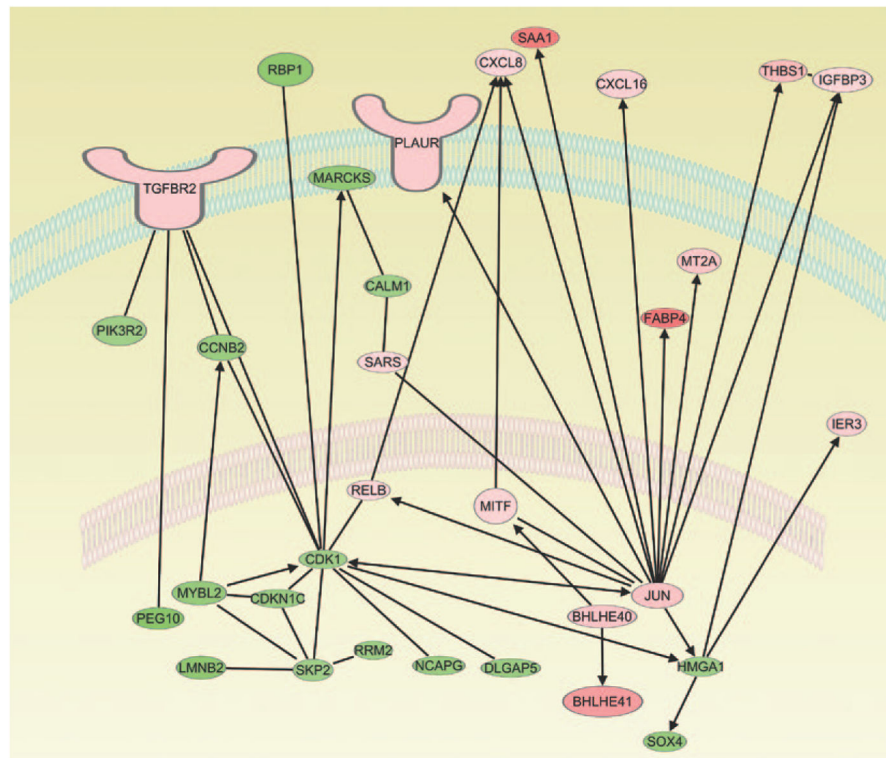


Figure 4. Network of genes represented by the genes altered during both developmental transitions, specifically in ductus arteriosus. The genes included are those which showed >1.5-fold change in expression. $N = 4$ in each group; $P < 0.05$.

Table 1

Genes altered more than twofold in ductus arteriosus (not in aorta) in response to developmental transition.

Gene symbol		136 d/97 d	NB/136 d
DES	Desmin	7.61	2.71
FGL2	Fibrinogen-like 2	5.21	2.31
FABP4	Fatty acid binding protein 4	5.05	4.61
SAA1	Serum amyloid A1	4.83	70.79
HR	Hairless homolog	3.92	5.67
BHLHE41	Basic helix-loop-helix family, member e41	3.59	1.60
ANKRD1	Ankyrin repeat domain 1 (cardiac muscle)	3.54	4.10
APOC2	Apolipoprotein C-II	2.71	2.43
PDK4	Pyruvate dehydrogenase kinase, isozyme 4	2.66	14.94
TP53INP2	Tumor protein p53 inducible nuclear protein 2	2.57	2.38
HKR1	HKR1, GLI-Kruppel zinc finger family member	2.43	2.42
SMOC2	SPARC related modular calcium binding 2	2.39	2.67
THBS1	Thrombospondin 1	2.39	4.11
LRRFIP1	Leucine rich repeat (in FLII) interacting protein 1	2.34	2.99
MAOA	Monoamine oxidase A	2.24	2.70
GSTENG00015013001	Shotgun Sequence SCAF14542	2.21	2.51
MT1A	Metallothionein 1A	2.18	221.19
RAMP1	Receptor (G protein-coupled) activity modifying protein 1	2.17	1.78
TRIB1	Tribbles homolog 1	2.16	2.31
SAMD4A	Sterile alpha motif domain containing 4A	2.15	1.56
CD9	CD9 molecule	2.14	1.52
JUN	Jun proto-oncogene	2.13	0.20
BHLHE40	Basic helix-loop-helix family, member e40	2.11	9.81
TL	Transcribed Locus (unknown protein)	2.11	1.96
MT2A	Metallothionein 2A	2.04	32.49
TMOD1	Tropomodulin 1	2.00	2.21
KLHDC10	Kelch domain containing 10	0.49	0.56
TNFRSF13C	Tumor necrosis factor receptor superfamily, member 13C	0.49	0.49
CDCA7	Cell division cycle associated 7	0.49	0.45
PEG10	Paternally expressed 10	0.49	0.55
PEG3	Paternally expressed 3	0.43	0.55
NRK	NIK related kinase	0.40	0.20
RPS24	Ribosomal protein S24	0.32	0.52
CTHRC1	Collagen triple helix repeat containing 1	0.32	0.08

Table 2 Chief upstream regulators which are known to produce similar gene expression changes as observed in the present dataset

Upstream regulator	Molecule type	Predicted activation state	Activation z-score	P value of overlap	Target molecules in dataset
CD40LG	Cytokine	Activated	2.2	1.09E-03	CXCL8, JUN, MARCKS, MT2A, PLAUR, RELB, TNFRSF13C
CDKN2A	Transcription regulator	Activated	2.4	1.11E-04	ASF1B, CDK1, JUN, MYBL2, PEG3, RRM2, SKP2
CEBPA	Transcription regulator	Activated	2.6	1.26E-07	CCNB2, CH13L1, CXCL8, FABP4, HMGAI, IER3, IGFBP3, JUN, MT2A, MYBL2, SAA1, TRIB1
Cisplatin	Chemical drug	Activated	2.2	4.10E-09	ANKRD1, BHLHE41, CD53, CDK1, CXCL8, FABP4, IER3, IGFBP3, JUN, MAOA, MARCKS, PDK4, RRM2, THBS1, TRIO, TYMS
CTNNB1	Transcription regulator	Activated	2.0	4.27E-06	BHLHE40, CALM1, CTHRC1, CXCL8, FABP4, JUN, MITF, PDE4B, PLAUR, SAA1, SFRP4, SOX4
EDN1	Cytokine	Activated	2.4	1.41E-04	CDK1, CXCL8, JUN, MITF, PLAUR, THBS1
FOS	Transcription regulator	Activated	2.4	1.58E-06	CH13L1, CXCL16, CXCL8, FABP4, JUN, MAOA, MT1A, MT2A, PLAUR, RBP1, RPS24, SFRP4
HIF1A	Transcription regulator	Activated	2.6	9.63E-05	BHLHE40, BHLHE41, CXCL8, FZD2, IGFBP3, JUN, MITF, PLAUR
Hydrogen peroxide	Chemical drug	Activated	2.4	1.99E-03	ANKRD1, CDK1, CXCL8, FZD2, JUN, MITF, PLAUR
IL1B	Cytokine	Activated	2.3	6.88E-06	APOC2, CH13L1, CXCL8, HMGAI, IER3, IGFBP3, JUN, LCP1, MT2A, PDE4B, RELB, SAA1, TGFB2, THBS1
IL2	Cytokine	Activated	2.2	4.34E-03	BHLHE40, CDKN1C, CXCL8, IER3, JUN, PDE4B, TNFRSF13C
L-triiodothyronine	Chemical drug	Activated	2.2	1.33E-02	APOC2, FABP4, HR, IGFBP3, PDK4
Lipopolysaccharide	Chemical drug	Activated	2.1	2.01E-10	APOC2, AZGP1, CALM1, CCNB2, CD53, CD9, CH13L1, CXCL16, CXCL8, FABP4, HMGAI, IER3, IGFBP3, JUN, KCNAB2, LRRFP1, MARCKS, MT2A, MYBL2, PDE4B, PDK4, PLAUR, RELB, SAA1, THBS1, TRIB1, UNC119
Methylprednisolone	Chemical drug	Activated	2.2	2.29E-02	CD9, FGL2, JUN, KCNAB2, PLAUR, TYRO3
NUPR1	Transcription regulator	Activated	2.4	1.81E-02	CCNB2, CXCL8, RELB, SAMD4A, SKP2, TRIB1
P38 MAPK	Group	Activated	2.5	6.11E-05	CXCL8, DES, JUN, MITF, PLAUR, RBP1, THBS1, TRIB1
Paclitaxel	Chemical drug	Activated	2.6	1.41E-09	BHLHE40, BHLHE41, CD53, CXCL8, IER3, IGFBP3, JUN, LCP1, NNAT, PLAUR, TGFB2, THBS1
PDX1	Transcription regulator	Activated	2.0	7.54E-04	IER3, IGFBP3, JUN, MITF, PDE4B
RBI	Transcription regulator	Activated	2.2	9.43E-05	ASF1B, CDK1, FABP4, MYBL2, RRM2, SKP2, TYMS
RELA	Transcription regulator	Activated	2.0	6.36E-04	ANKRD1, CH13L1, CXCL8, IER3, JUN, RELB, SAA1

Upstream regulator	Molecule type	Predicted activation state	Activation z-score	P value of overlap	Target molecules in dataset
TNF	Cytokine	Activated	2.6	9.19E-07	APOC2, BHLHE40, BHLHE41, CHI3L1, CXCL16, CXCL8, FABP4, IER3, IGFBP3, JUN, MT1A, PDE4B, PLAUR, RBP1, RELB, RR M2, SAA1, SAMD4A, SOX4, TGFB2, THBS1
TNFSF11	Cytokine	Activated	2.2	3.59E-03	CXCL8, IER3, JUN, PLAUR, RELB
MYC	Transcription regulator	Inhibited	-3.0	2.72E-09	ACSL4, CCNB2, CD9, CDCA7, CDK1, CXCL8, FABP4, HMGAI, IER3, JUN, MITF, PEG3, PLAUR, RBP1, RRM2, SKP2, TGFB2, THBS1, TYMS, UNC119
NR3C1	Ligand-dependent nuclear receptor	Inhibited	-2.6	1.29E-05	BHLHE40, CDKN1C, CXCL8, IER3, JUN, MAOA, MYOC, PDE4B, RERE, SOX4, THBS1, ZNF704
SB203580	Chemical kinase inhibitor	Inhibited	-2.7	8.54E-05	CXCL8, IER3, IGFBP3, JUN, MITF, PDE4B, PLAUR, THBS1

Table 3

Functional annotation of the downregulated genes with ductus arteriosus developmental transition

Symbol	Entrez gene name	Type(s)
SKA1	Spindle and kinetochore associated complex subunit 1	Cell division
ZWINT	ZW10 interacting kinetochore protein	Cell division
KNTC1	Kinetochore associated 1	Cell division
NCAPG	Non-SMC condensin I complex, subunit G	Cell division
CENPH	Centromere protein H	Cell division
CCNB2	Cyclin B2	Cell division
SKP2	S-phase kinase-associated protein 2, E3 ubiquitin protein ligase	Enzyme
RRM2	Ribonucleotide reductase M2	Enzyme
RAD54L	RAD54-like (<i>S. cerevisiae</i>)	Enzyme
NDUFA2	NADH dehydrogenase (ubiquinone) 1 alpha subcomplex, 2, 8 kDa	Enzyme
CA11	Carbonic anhydrase XI	Enzyme
RASL11B	RAS-like, family 11, member B	Enzyme
TYMS	Thymidylate synthetase	Enzyme
CALM1	Calmodulin 1 (phosphorylase kinase, delta)	Enzyme regulator
FZD2	Frizzled class receptor 2	G protein-coupled receptor
KCNAB2	Potassium voltage-gated channel, shaker-related subfamily, beta member 2	Ion channel
CDK1	Cyclin-dependent kinase 1	Kinase
PIK3R2	Phosphoinositide-3-kinase, regulatory subunit 2 (beta)	Kinase
TYRO3	TYRO3 protein tyrosine kinase	Kinase
TRIO	Trio Rho guanine nucleotide exchange factor	Kinase
NRK	NIK related kinase	Kinase
CDKN1C	Cyclin-dependent kinase inhibitor 1C (p57, Kip2)	Kinase regulator
DLGAP5	Discs, large (<i>Drosophila</i>) homolog-associated protein 5	Phosphatase
UNC119	Unc-119 homolog (<i>C. elegans</i>)	Protein trafficking
PTGFRN	Prostaglandin F2 receptor inhibitor	Receptor regulator
FNDC5	Fibronectin type III domain containing 5	Secreted protein
KLHDC10	Kelch domain containing 10	Signal transduction
SDC3	Syndecan 3	Structural protein
EML1	Echinoderm microtubule associated protein like 1	Structural protein
NRM	Nurim (nuclear envelope membrane protein)	Structural protein
RMI2	RecQ mediated genome instability 2	Structural protein
MARCKS	Myristoylated alanine-rich protein kinase C substrate	Structural protein
LMNB2	Lamin B2	Structural protein
CTHRC1	Collagen triple helix repeat containing 1	Structural protein
HMGA1	High mobility group AT-hook 1	Transcription regulator
ZNF704	Zinc finger protein 704	Transcription regulator
HMG1	High mobility group nucleosome binding domain 1	Transcription regulator
ZNF532	Zinc finger protein 532	Transcription regulator
SOX4	SRY (sex determining region Y)-box 4	Transcription regulator

Symbol	Entrez gene name	Type(s)
MYBL2	v-myb avian myeloblastosis viral oncogene homolog-like 2	Transcription regulator
ASF1B	Anti-silencing function 1B histone chaperone	Transcription regulator
CDCA7	Cell division cycle associated 7	Transcription regulator
PEG10	Paternally expressed 10	Transcription regulator
PEG3	Paternally expressed 3	Transcription regulator
RPS24	Ribosomal protein S24	Translational regulator
SFRP4	Secreted frizzled-related protein 4	Transmembrane receptor
TNFRSF13C	Tumor necrosis factor receptor superfamily, member 13C	Transmembrane receptor
SLC2A8	Solute carrier family 2 (facilitated glucose transporter), member 8	Transporter
AZGP1	Alpha-2-glycoprotein 1, zinc-binding	Transporter
RBP1	Retinol binding protein 1, cellular	Transporter
NNAT	Neuronatin	Transporter

Table 4

Functional annotations of the upregulated genes with ductus arteriosus developmental transition

Symbol	Entrez gene name	Type(s)
CXCL16	Chemokine (C-X-C motif) ligand 16	Cytokine
CXCL8	Chemokine (C-X-C motif) ligand 8	Cytokine
DES	Desmin	Cytoskeleton
MYOC	Myocilin, trabecular meshwork inducible glucocorticoid response	Cytoskeleton
PDK4	Pyruvate dehydrogenase kinase, isozyme 4	Enzyme
MAOA	Monoamine oxidase A	Enzyme
TRIB1	Tribbles pseudokinase 1	Enzyme
TMOD1	Tropomodulin 1	Enzyme
CHI3L1	Chitinase 3-like 1 (cartilage glycoprotein-39)	Enzyme
PDE4B	Phosphodiesterase 4B, cAMP-specific	Enzyme
ACSL4	Acyl-CoA synthetase long-chain family member 4	Enzyme
SARS	Seryl-tRNA synthetase	Enzyme
FGL2	Fibrinogen-like 2	Extracellular ligand
SMOC2	SPARC related modular calcium binding 2	Extracellular ligand
THBS1	Thrombospondin 1	Extracellular ligand
IGFBP3	Insulin-like growth factor binding protein 3	Extracellular ligand
FABP4	Fatty acid binding protein 4, adipocyte	Membrane receptor/protein
SAA1	Serum amyloid A1	Membrane receptor/protein
APOC2	Apolipoprotein C-II	Membrane receptor/protein
RAMP1	Receptor (G protein-coupled) activity modifying protein 1	Membrane receptor/protein
CD9	CD9 molecule	Membrane receptor/protein
PLAUR	Plasminogen activator, urokinase receptor	Membrane receptor/protein
TGFBR2	Transforming growth factor, beta receptor II (70/80 kDa)	Membrane receptor/protein
CD53	CD53 molecule	Membrane receptor/protein
MT1A	Metallothionein 1A	Metabolic protein
MT2A	Metallothionein 2A	Metabolic protein
LCP1	Lymphocyte cytosolic protein 1 (L-plastin)	Metabolic protein
ATG2A	Autophagy related 2A	Metabolic protein
HR	Hair growth associated	Transcription regulator
BHLHE41	Basic helix-loop-helix family, member e41	Transcription regulator
ANKRD1	Ankyrin repeat domain 1 (cardiac muscle)	Transcription regulator
TP53INP2	Tumor protein p53 inducible nuclear protein 2	Transcription regulator
HKR1	HKR1, GLI-Kruppel zinc finger family member	Transcription regulator
LRRFIP1	Leucine rich repeat (in FLII) interacting protein 1	Transcription regulator
JUN	Jun proto-oncogene	Transcription regulator
BHLHE40	Basic helix-loop-helix family, member e40	Transcription regulator
IER3	Immediate early response 3	Transcription regulator
RERE	Arginine-glutamic acid dipeptide (RE) repeats	Transcription regulator
MITF	Microphthalmia-associated transcription factor	Transcription regulator

Symbol	Entrez gene name	Type(s)
RELB	v-rel avian reticuloendotheliosis viral oncogene homolog B	Transcription regulator
SAMD4A	Sterile alpha motif domain containing 4A	Translation regulator
KIAA1671	KIAA1671	Uncharacterized

Author Manuscript

Author Manuscript

Author Manuscript

Author Manuscript

Table 5

Genes common in this study and a study in rat ductus

Gene symbol		136 d/97 d	Rat DA21/DA19
DES	Desmin	7.61	4.13773421
PDK4	Pyruvate dehydrogenase kinase, isozyme 4	2.66	2.566222222
MAOA	Monoamine oxidase A	2.24	2.175630978
CD9	CD9 molecule	2.14	1.525717393
JUN	Jun proto-oncogene	2.13	2.888589354
BHLHE40	Basic helix-loop-helix family, member e40	2.11	1.522832723
IER3	Immediate early response 3	1.79	1.726213221
PDE4B	Phosphodiesterase 4B, cAMP-specific	1.70	2.505808477
ACSL4	Acyl-CoA synthetase long-chain family member 4	1.57	1.657947377
IGFBP3	Insulin-like growth factor binding protein 3	1.52	1.579121148
CDKN1C	Cyclin-dependent kinase inhibitor 1C (p57, Kip2)	0.61	0.407179049
AZGP1	Alpha-2-glycoprotein 1, zinc-binding	0.60	0.507969152